Multicritical point and unified description of broken-symmetry phases in spin-$\frac{1}{2}$ antiferromagnets on a square lattice

Oğuz Türker and Kun Yang ⊙

National High Magnetic Field Laboratory and Department of Physics, Florida State University, Tallahassee, Florida 32306, USA

We show that several distinct broken-symmetry phases in a spin-$\frac{1}{2}$ antiferromagnet on a square lattice with easy-plane anisotropy, including valence bond solid, chiral spin liquid, and the XY-ordered state, can all be accessed by perturbing a multicritical point with two massless Dirac fermions coupled to a level-one Chern-Simons gauge field. This allows for a unified description of these phases, as well as the phase transitions between them. In a specific phase transition, our analysis provides a lattice realization of one of the recently proposed fermion-boson dualities, thus lending support to it. We also briefly discuss the relation between our paper and the long-sought deconfined criticality in such systems.

I. INTRODUCTION

Two-dimensional (2D) spin-$\frac{1}{2}$ antiferromagnets can support a large variety of phases, many of them break spin-rotation and/or lattice symmetries. Spin liquids [1], which break none of these symmetries, have been the focus of much recent research activity. They come in many different types as well. One such type, known as chiral spin liquid that breaks time-reversal symmetry, will be of particular relevance to our discussion below. Needless to say, quantum phase transitions among all these phases are also of strong interest.

Broken symmetry phases are traditionally described in Ginzburg-Landau theory, which is a field theory written in terms of the local order parameter associated with the spontaneously broken symmetry (see, e.g., Ref. [2]). In such descriptions, phases with different broken symmetries are described using different order parameter fields, and direct second-order transitions between them require fine-tuning. Instead, the more generic situations are first-order transitions or intermediate phases where both types of orders coexist. In Ref. [3], Senthil *et al.* argue that such descriptions miss the possibility of deconfined criticality, which is a critical point separating two different broken symmetries facilitating a direct second-order transition between them. Such novel quantum criticality can only be captured in a field theory that describe both types of broken symmetries on equal footing. Specifically, they argue that such deconfined critical points separate the Neel ordered and valence bond solid (VBS) phases of 2D spin-$\frac{1}{2}$ antiferromagnets, which break spin-rotation and lattice translation symmetry, respectively. In the appropriate field theory, the two symmetry-breaking order parameters are dual to each other and thus afford a unified description. Numerous attempts have been made to identify such deconfined critical points, with inconclusive outcomes thus far (see Refs. [4,5] for recent attempts for the Heisenberg and XY symmetry classes, respectively, and references therein).

While it is *not* our goal to resolve the fate of deconfined criticality, our work is motivated by the line of thoughts that lead to it. To this end, we seek to find a field theory that provides a unified description of relevant phases in this description and beyond. We find by perturbing a theory of two massless Dirac fermions coupled to a single level-one Chern-Simons (CS) gauge field, we can reach the XY-ordered (we only consider 2D spin-$\frac{1}{2}$ antiferromagnets with easy-plane anisotropy in this paper) VBS, chiral spin liquid, and an Ising Neel state in which the Neel order is along the z direction despite the easy-plane anisotropy (which is possible in the presence of frustration). Within this description, a direct second-order transition between the XY-ordered phase and the VBS or Ising Neel phase must go through this massless point, which requires fine-tuning.

The remainder of the paper is organized as follows. In Sec. II, we introduce the spin-$\frac{1}{2}$ XY model and arrive at the multicritical point by attaching a flux quantum to each hard-core boson that represents an up spin, and perform a mean-field approximation to smear out the flux. This results in two massless Dirac fermions coupled to a level-one CS field. In Sec. III, we discuss the phases that result when various mass terms are added to perturb this critical point. In Sec. IV, we discuss how the mass terms responsible for spontaneous lattice symmetry breaking are generated by fermion interactions. Section V is devoted to deriving the dual bosonic theory of the multicritical point, where we also make comparison with the existing theory of deconfined criticality. A brief summary is offered in Sec. VI.

II. MODEL AND COMPOSITE FERMION MEAN-FIELD APPROXIMATION

We consider the following spin-$\frac{1}{2}$ Hamiltonian on the square lattice:

$$H = -\sum_{<ij>} \left(S_i^x S_j^x + S_i^y S_j^y \right) + \cdots \tag{1}$$
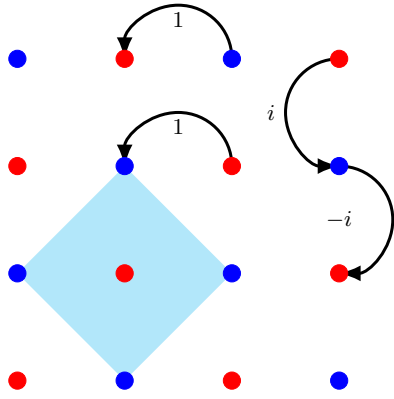
$$= H_0 + \cdots, \tag{2}$$

FIG. 1. Gauge choice for fermion hopping phases. The magnetic unit cell contains two squares, two lattice sites (one each from A and B sublattices), and a total of 2π flux. For bonds with imaginary phases, the phase corresponds to hopping in the direction of the error.

where $\langle ij \rangle$ stands for nearest neighbors and the ellipsis represents generic additional couplings that respect the XY rotation symmetry and all lattice symmetries unless noted otherwise. Note that the minus sign means the XY coupling is ferromagnetic instead of antiferromagnetic; the two are equivalent under a π rotation along the z direction for one of the two sublattices. The advantage of considering the ferromagnetic XY coupling is the XY-ordered phase only breaks the $O(2)$ spin rotation symmetry, but none of the lattice symmetries. This makes the discussion of broken symmetries in various phases simpler below. The antiferromagnetic nature of Eq. (1) is thus hidden in the ellipsis, which include S^z and further neighbor couplings between XY spins in the same sublattice.

We can map half-spin ladder operators to annihilation and creation operators of the hard-core bosons. Accordingly, the nearest-neighbor XY spin coupling in Eq. (1) becomes nearest-neighbor boson hopping,

$$H_0 = -\frac{1}{2} \sum_{\langle ij \rangle} (b_i^\dagger b_j + b_j^\dagger b_i), \qquad (3)$$

and the ground state has half filling in the absence of a net magnetization along the z direction. We will use the spin and boson representations interchangeably below.

To proceed, we map the hard-core bosons to composite fermions (CFs) attached to a flux quantum by coupling them with pure CS theory in lattice, and then make a mean-field approximation to spread out the flux uniformly that results in a π (or half) flux per plaquette [6]. With the gauge choice of Fig. 1, the resultant band Hamiltonian takes the form

$$h_{\boldsymbol{k}} = \begin{pmatrix} 0 & \sin k_x + i \sin k_y \\ \sin k_x - i \sin k_y & 0 \end{pmatrix}, \qquad (4)$$

in which $\boldsymbol{k}$ is the lattice momentum. Importantly, we have two Dirac points at $(0, 0)$ and $(\pi, 0)$ where the two bands meet. In the ground state, the lower band is filled while the upper band is empty, so the chemical potential coincides with the Dirac points. Thus, the low-energy physics of the system at this level of approximation is described by two species of massless Dirac fermions coupled to a *single* CS gauge field:

$$\mathcal{L} = i \bar{\Psi} \slashed{D} \Psi + \mathcal{L}_{\text{CS}}[a] + \cdots, \qquad (5)$$

where

$$\mathcal{L}_{\text{CS}}[a] = \frac{1}{4\pi} \epsilon^{\mu\nu\lambda} a_\mu \partial_\nu a_\lambda = a \wedge da \qquad (6)$$

is the level-one CS term, $\Psi = (\psi_1, \psi_2)^T$ combines the two Dirac fields [7] where ψ_i are two-component Dirac spinors, the slash notation is defined for a general three-vector b_μ as $\slashed{b} = \gamma^\mu b_\mu$, where γ^μ are two by two Dirac matrices obeying the Clifford algebra $\{\gamma^\mu, \gamma^\nu\} = 2\eta^{\mu\nu}$, where $\eta^{\mu\nu}$ is the metric of the Minkowski $2 + 1$ space-time and $\eta^{\mu\nu} = \text{diag}(+, -, -)$, which will be used for raising and lowering the indices throughout the paper and $\{, \}$ is the anticommutator. $D_\mu = \partial_\mu - i a_\mu - i A_\mu$ includes coupling to both the dynamic field a_μ and background gauge field A_μ, and the ellipsis represents the less relevant terms like the Maxwell term of a. Equation (5) is the same theory discussed in Ref. [8] in a closely related context. As we demonstrate below, a variety of interesting phases supported by Eq. (1) can be accessed by perturbing Eq. (4) with various mass terms for the Dirac fermions.

III. DIRAC MASS TERMS AND CORRESPONDING BROKEN SYMMETRY PHASES

The most general mass term that couples the two Dirac points takes the form $\bar{\Psi} M \Psi$, where

$$M = m_0 \mathbb{1} + m_1 \sigma_1 + m_2 \sigma_2 + m_3 \sigma_3 = m_0 \mathbb{1} + \boldsymbol{m} \cdot \boldsymbol{\sigma} \qquad (7)$$

is a two-by-two Hermitian matrix. In the following, we discuss how such mass terms can be generated beyond the mean-field Hamiltonian Eq. (4) and what phases they generate once added to the critical theory Eq. (5).

A. Uniform mass m_0

We first consider next-nearest-neighbor XY coupling,

$$H_{\text{nnn}} = J' \sum_{\langle\langle ij \rangle\rangle} \left(S_i^x S_j^x + S_i^y S_j^y \right), \qquad (8)$$

$$= J' \sum_{\langle\langle ij \rangle\rangle} (b_i^\dagger b_j + b_j^\dagger b_i), \qquad (9)$$

where $\langle\langle ij \rangle\rangle$ stands for next-nearest neighbors. Within the mean-field approximation and using the gauge choice that hopping between A sublattice sites have phase $+1$ and that between B sublattice sites have phase -1 results in a term of the form

$$h'_{\boldsymbol{k}} = 2J' \begin{pmatrix} \cos k_x \cos k_y & 0 \\ 0 & -\cos k_x \cos k_y \end{pmatrix}, \qquad (10)$$

resulting in a uniform mass term with $m_0 = 2J'$, while $\boldsymbol{m} = 0$.

We now analyze the phases stabilized by $m_0 \neq 0$. Since the fermions are massive, they can be integrated out. This results in a CS term $\text{sgn}(m_0)\mathcal{L}_{\text{CS}}[A + a]$ whose sign depends on that of m_0 or, equivalently, J', which needs to be combined with the original CS term for a in Eq. (5). We analyze the two cases separately.

(i) $m_0 < 0$. In this case, we have

$$\mathcal{L}_{\text{eff}}[a, A] = \mathcal{L}_{\text{CS}}[a] - \mathcal{L}_{\text{CS}}[a + A] = -2a \wedge dA - \mathcal{L}_{\text{CS}}[A]. \qquad (11)$$

Since the CS coupling of a gets canceled, we are left with a linear coupling between a and A. Further integrating out a yields a constraint $dA = 0$. This corresponds to a Meissner response of the hard core bosons, indicating they are in a superfluid phase that spontaneously breaks the U(1) symmetry that corresponds to charge conservation [8]. For the original spin-$\frac{1}{2}$ Hamiltonian Eq. (1), this is the XY-ordered phase [6].

(ii) $m_0 > 0$. In this case, we have

$$\mathcal{L}_{\text{eff}}[a, A] = \mathcal{L}_{\text{CS}}[a] + \mathcal{L}_{\text{CS}}[a + A]$$
$$= 2a \wedge da + 2a \wedge dA + \mathcal{L}_{\text{CS}}[A]. \quad (12)$$

Further integrating out a yields

$$\mathcal{L}_{\text{eff}}[A] = -\tfrac{1}{2} A \wedge dA + \mathcal{L}_{\text{CS}}[A] = \tfrac{1}{2} \mathcal{L}_{\text{CS}}[A]. \quad (13)$$

This is a fractional quantum Hall response corresponding to the $\nu = \frac{1}{2}$ Laughlin state for bosons [8]. In the original spin model, this corresponds to the Kalmeyer-Laughlin chiral spin liquid (CSL) state, in which time-reversal symmetry is spontaneously broken. The same result was obtained earlier on triangular and Kagomé lattices with antiferromagnetic nearest-neighbor XY coupling only [9].

It should be noted that while the mean-field Hamiltonian Eq. (4) suggests that the nearest-neighbor XY model is a critical point separating the CSL and XY-ordered phases, it is known that its ground state is actually XY ordered. As discussed in Ref. [6], fluctuation effects beyond the mean-field approximation tend to generate a negative m_0. We thus need a positive J', which *frustrates* the XY order, to reduce the magnitude of the dynamically generated negative mass, and eventually drive the system into the CSL phase. It would be very interesting to study the spin-$\frac{1}{2}$ XY model with the frustrating next-nearest-neighbor J' coupling to see if such a transition exists.

B. Staggered mass m_3

We call m_3 in Eq. (7) staggered mass because it gives rise to masses of opposite sign to the two Dirac fermions. Interestingly, it comes from a staggered potential coupled to the hardcore boson density (which is equal to the CF density),

$$v = m_3 \sum_i (-1)^i b_i^\dagger b_i = 2m_3 \sum_i (-1)^i S_i^z + \text{const}, \quad (14)$$

and the second equality above indicates it couples to the staggered magnetization along the z direction in the original spin language. Such a mass could come from spontaneous development of staggered magnetization along the z direction [6], which breaks lattice translation symmetry *spontaneously*. We call the resultant phase an Ising-ordered phase (to be distinguished from the XY-ordered phase discussed earlier). m_3 could also come from an external potential with wave vector (π, π), which breaks lattice translation symmetry *explicitly*.

Regardless of its origin, in the presence of m_3 the Dirac fermions can again be integrated out. Since they have opposite masses, the CS terms they generate cancel. Further integrating out a with the existing CS term thus generates no term involving A, indicating the state has no (nontrivial) electromagnetic response. This is thus a Mott insulator state for the hardcore bosons.
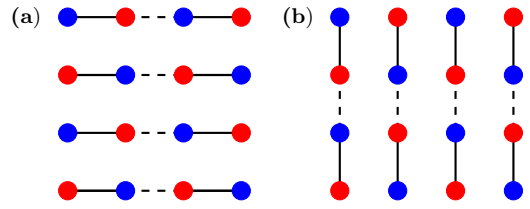

FIG. 2. Column valence bond solid (VBS) patterns. Solid lines represent strengthened bonds while dashed lines represent weakened bonds. (a) The column VBS directed along x axis, carrying lattice momentum $(\pi, 0)$. (b) The column VBS, directed along y axis, carrying lattice momentum $(0, \pi)$.

Reference [6] was mainly concerned about the quantum phase transition from the XY-ordered to Ising-ordered state in the nearest-neighbor XXZ model, which is actually a first-order transition that occurs at the Heisenberg point. In the presence of frustration, like that induced by J', XY order gets suppressed and a direct second-order transition between them may be possible. Since m_3 breaks lattice translation symmetry, it must remain zero at this (putative) critical point. As a result, the transition must again be driven through the critical point described by Eq. (5), where m_0 vanishes and m_3 gets turned on simultaneously. This is different from the conclusion of Ref. [6], where the authors assumed the presence of both m_0 and m_3, resulting in masses $m_0 \pm m_3$ for the two Dirac fermions, and the critical point is reached at $m_0 = m_3$, where only one of the two Dirac fermions become massless,

$$\mathcal{L} = i\bar{\psi}\slashed{D}\psi + \mathcal{L}_{\text{CS}}[a] + \cdots, \quad (15)$$

where ψ is the field of this massless Dirac fermion. This same model was also discussed in Ref. [10].

From the discussions above, it becomes clear that for the theory [Eq. (15)] to be relevant, before the XY order is suppressed, the Ising order must be present already, due to either spontaneous or explicit breaking of lattice translation symmetry. We consider the latter for its simplicity. With a staggered lattice potential of the form [Eq. (14)], the unit cell of the square lattice gets doubled, and so does the boson filling from half to one per unit cell. We thus have a standard superfluid to Mott-Insulator transition in this case, which is described by the familiar $O(2)$ ϕ^4 theory. Our analysis thus support the recently proposed duality between Eq. (15) and the corresponding Wilson-Fisher fixed point [11].

C. Off-diagonal masses m_1 and m_2

As discussed above, the staggered mass m_3 breaks lattice translation symmetry and carries momentum (π, π). The off-diagonal mass terms m_1 and m_2 couple the two Dirac points and must carry momentum $(\pi, 0)$ or $(0, \pi)$. They thus break lattice translation symmetry in a different manner. As we demonstrate below, column VBS orders correspond to such symmetry breaking pattern and generates these masses.

VBS order, generated either spontaneously or explicitly, modulates the spin-spin coupling strength. We consider the most important column VBS patterns, which could align along either the x or y direction (see Fig. 2). It is immediately clear that they carry momenta $(\pi, 0)$ and $(0, \pi)$, respectively.
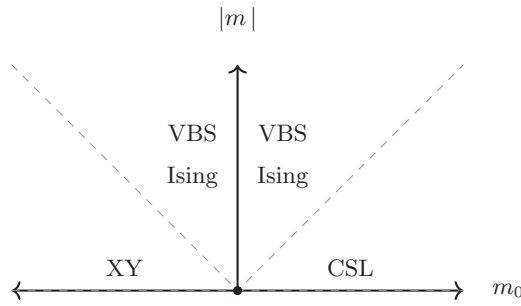
FIG. 3. Phase diagram parameterized by the mass matrix of Eq. (7). The dashed lines are second-order phase boundaries along which one of the eigenvalues of the mass matrix Eq. (7) vanishes. The origin (thick dot) is a multicritical point where the entire mass matrix Eq. (7) vanishes. See text for detailed description of phases and the symmetries they break.

A straightforward calculation yields $m_{2,3} = \delta$ for the patterns of Figs. 2(a) and 2(b), respectively, where δ is the bond modulation.

In the presence of m_2 and/or m_3, we can diagonalize the mass matrix Eq. (7) resulting in the same Dirac Hamiltonian as that of m_3 mass only. So the system has the same topological properties as well, and is in the Mott insulator phase.

D. Summary

When all masses are present, diagonalizing the mass matrix Eq. (7) yields

$$m = m_0 \pm \sqrt{m_1^2 + m_2^2 + m_3^2} = m_0 \pm |\boldsymbol{m}|, \qquad (16)$$

where $\boldsymbol{m} = (m_1, m_2, m_3)$. The resultant phase diagram, Fig. 3, looks similar to that of Ref. [8], although what we have here is actually a 4D phase diagram projected down to the 2D plane spanned by m_0 and $|\boldsymbol{m}|$. In particular, we note all components of $\boldsymbol{m}$ break lattice translation symmetry, but in different ways. On the other hand, m_0, while not breaking lattice translation symmetry, leads to phases that break $O(2)$ spin rotation symmetry or time-reversal symmetry when it dominates, in the same manner as discussed in Sec. III A.

In our description, the two perpendicular VBS order parameters give rise to the real and imaginary parts of the off-diagonal Dirac mass in Eq. (7). They thus naturally form a complex order parameter, consistent with an earlier study [3]. We find they can be further combined with stagger magnetization m_3 to form an $O(3)$ order parameter, and they cooperate to enhance the Mott gap; in other words, they are intertwined. On the other hand, they compete with the uniform mass m_0, and such competition leads to various quantum phase transitions. Despite such competition, our analysis suggests that all the phases that appear in Fig. 3 naturally appear near each other in a frustrated spin-$\frac{1}{2}$ model on the square lattice, in the neighborhood of a multicritical point described by Eq. (5).

IV. SPONTANEOUS BREAKING OF LATTICE SYMMETRY

From the perspective of the field theory Eq. (5), the massless point for both of the Dirac fermions (the origin in Fig. 3) is multicritical and the full mass matrix of Eq. (7) must be tuned to zero. For example a direct second-order transition from the XY phase to the VBS phase must go through this point, while a more generic situation is going through the coexisting region or a direct first-order transition. On the other hand, the masses $\boldsymbol{m}$ break lattice symmetries. Thus, unlike m_0, they are not tuning parameters, but are instead generated from (sufficiently) strong interactions that lead to spontaneous symmetry breaking. Accordingly, we consider the following four-Fermi (Gross-Neveu type) interaction:

$$\begin{aligned}
\mathcal{L}_{\mathrm{int}} = {} & \lambda_0[(\overline{\psi}_1\psi_1)^2 + (\overline{\psi}_2\psi_2)^2] + \lambda_1(\overline{\psi}_1\psi_1)(\overline{\psi}_2\psi_2) \\
& + \lambda_2(\overline{\psi}_1\psi_2)(\overline{\psi}_2\psi_1) + \lambda_3(\overline{\psi}_1\psi_2)^2 + \lambda_3^*(\overline{\psi}_2\psi_1)^2.
\end{aligned}$$
$$(17)$$

It is clear that a positive λ_1 favors m_3, while a negative λ_2 and any λ_3 favor $m_{1,2}$. We can introduce Hubbard-Stratonovich fields Φ to decouple these interactions, resulting in a Yukawa type of coupling

$$\mathcal{L}_Y = \bar{\Psi}\Phi\Psi, \qquad (18)$$

where

$$\Phi = \phi_0\mathbb{1} + \phi_1\sigma_1 + \phi_2\sigma_2 + \phi_3\sigma_3. \qquad (19)$$

Obviously $\boldsymbol{\phi} = (\phi_1, \phi_2, \phi_3)$ is an order parameter field describing the broken lattice symmetry.

The ordering transition is described by an effective field theory in terms of $\boldsymbol{\phi}$ obtained from integrating out Ψ. This can be done under the generic situation of $m_0 \neq 0$. Such a transition, if continuous, takes the system from the XY/CSL phase to a mixed phase where spontaneously broken XY/time-reversal symmetry coexist with spontaneously broken lattice symmetry. A direct continuous transition from the XY phase to the VBS phase, however, again requires fine-tuning m_0 to zero; in this case, the Dirac fermions are massless and cannot be integrated out perturbatively.

Returning to the generic situation of $m_0 \neq 0$, to determine the order of transition this effective theory describes at the mean-field level, we are interested in the sign of the prefactor of the $|\boldsymbol{\phi}|^4$ term. Let us denote this prefactor as β_4. We can calculate it diagrammatically. For notational simplicity, we focus on the ϕ_3 term in Eq. (19) as a representative of $\boldsymbol{\phi}$; the conclusions below are general. Also, we assume a uniform $|\boldsymbol{\phi}| = m$.

The Feynman rules we use are given in Fig. 4. The diagrams up to two loops that contribute to β_4 are shown in Fig. 5 [12]. The expansion in the number of loops is equivalent to a weak coupling expansion in terms of the coupling constant between fermions and CS gauge field [13], the inverse of the square root of the absolute value of the CS level. We do not show this coupling constant explicitly in our calculations for brevity of the notation. We adopt a renormalized perturbation theory approach, in which we replace the bare mass m_0 with renormalized mass m_r in the free propagators and compensate this by adding mass and field-strength renormalization counterterms.

Before the quantitative computation of β_4, we can have a qualitative discussion on what to expect. The dimension of the β_4 has an inverse mass dimension, i.e., $[\beta_4] = [m^{-1}]$. On the other hand, the only dimensionful free parameter in the theory (and relevant Feynman diagrams that generate β_4) is the mass m_r. We thus expect β_4 is inversely proportional to the mass. We will calculate this proportionality constant below.

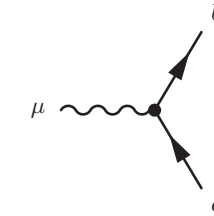We start with calculating the one-loop contribution D_1 which is shown in Fig. 5:

$$D_1 = -\frac{1}{4}\text{tr}\left[\int \frac{d^3p}{(2\pi)^3}\frac{(i(\not{p}-m_r))^4}{(p^2-m_r^2)^4+i\epsilon}\right]$$

$$= -\frac{1}{4}\text{tr}\left[\int \frac{d^3p}{(2\pi)^3}\frac{p^4-4p^2 m_r\not{p}+6p^2m^2-4\not{p}m_r^3+m_r^4}{(p^2-m_r^2)^4+i\epsilon}\right]$$

$$= -\frac{2}{4}\int \frac{d^3p}{(2\pi)^3}\frac{p^4+6p^2m_r^2+m_r^4}{(p^2-m_r^2)^4+i\epsilon}, \tag{20}$$

which, after Wick rotating to Euclidean coordinates $p_E^\mu = p_{E\mu} = (-ip^0, \boldsymbol{p})$ and $\not{p} = -i\not{p}_E$, becomes

$$D_1 = -\frac{i}{2}\frac{1}{|m_r|}\int \frac{d^3p_E}{(2\pi)^3}\frac{p_E^4-6p_E^2+1}{((p_E)^2+1)^4}. \tag{21}$$

Using the integral identities given in Appendix with $n=4$, $d=3$ we find

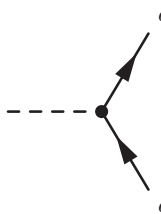$$D_1 = -\frac{i}{2}\frac{\Gamma(\frac{1}{2})}{(4\pi)^{3/2}\Gamma(4)}\left(\frac{1}{|m_r|}\right)\left[\frac{15}{4}-\frac{18}{4}+\frac{3}{4}\right],$$

$$= 0. \tag{22}$$

$$\mu \;\;\sim\!\!\sim\!\!\sim\;\; {}^{b}_{a} \qquad = i\gamma^\mu \delta_{ab} \tag{20a}$$

$$\mu \;\;\sim\!\!\sim\!\!\sim\;\; \nu = -2\pi\epsilon^{\mu\nu\alpha}\frac{p_\alpha}{p^2+i\epsilon} \tag{20b}$$

$$\text{-- -- --}\;\;{}^{a}_{a} \qquad = i(\delta_{a1}-\delta_{a2}) \tag{20c}$$
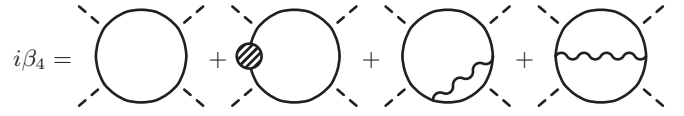
$$a \longrightarrow b = \frac{i}{\not{p}+m_r+i\epsilon}\delta_{ab} \tag{20d}$$

$$\text{---}\!\times\!\text{---} \qquad = i(\not{p}\delta_2+\delta m_r) \tag{20e}$$

FIG. 4. Feynman rules of our model, where a, b denote fermion flavors. Dashed lines represent ϕ_3, solid lines represent fermions, and curly lines represent the gauge field a_μ (we use Landau gauge), and finally the cross is the counterterm which we denote as D_5, where δ_2 is the fermion field strength renormalization counterterm and δ_m is the mass counterterm (see also Fig. 6). We will drop the arrows in the fermionic lines in the rest of the paper to have less cluttered diagrams.

FIG. 5. Diagrammatic representation of the β_4 up to two loops. We denote these diagrams, respectively, from left to right as, D_1, D_2, D_3, D_4 and the shaded blob is the self-energy which is shown in Fig. 6.

As a preparation for the calculation of the two-loop diagrams, we first calculate the fermion self-energy, Σ, up to leading (one-loop) order in gauge coupling,

$$-i\Sigma = -i\Sigma_2 + D_5, \tag{23}$$

where $-i\Sigma_2$ is shown in Fig. 6 and given as

$$-i\Sigma_2 = 2\pi i \int \frac{d^3q}{(2\pi)^3}\frac{\gamma_\mu(\not{q}-m_r)\gamma_\nu}{q^2-m_r^2+i\epsilon}\frac{\epsilon^{\mu\nu\alpha}(p-q)_\alpha}{(p-q)^2+i\epsilon}, \tag{24}$$

and D_5 is the corresponding counter term. Equation (24) has a linear UV divergence. We can remove this by applying Pauli-Villars regularization, which is equivalent to the following
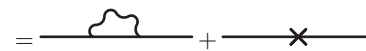
$$-i\Sigma_2 = \quad\text{---}\!\frown\!\text{---} \tag{24a}$$

$$\Gamma_1 = \quad\text{---}\!\frown\!\text{---} \tag{24b}$$

$$\Gamma_2 = \quad\text{---}\!\frown\!\text{---} \tag{24c}$$

$$D_5 = \quad\text{---}\!\times\!\text{---} \tag{24d}$$

$$-i\Sigma = \quad\text{---}\!\bigcirc\!\text{---}$$

$$= \quad\text{---}\!\frown\!\text{---} + \text{---}\!\times\!\text{---} \tag{24e}$$

FIG. 6. Electron self-energy and vertex corrections. Respectively, we have electron self-energy, $-i\Sigma_2$, the vertex correction Γ_1, Γ_2, and the counterterms D_5. Those are also amputated.

substitution [14] in Eq. (24):

$$\frac{1}{(p-q)^2} \rightarrow \frac{1}{(p-q)^2} - \frac{1}{(p-q)^2 - \Lambda^2}, \quad (25)$$

where Λ is the cutoff. Next, we use Feynman parameters to bring the denominator of Eq. (24) in a spherically symmetric form by using the identity [14]

$$\frac{1}{(q^2 - m_r^2)^n (p-q)^2} = \int_0^1 dx \frac{n(1-x)^{n-1}}{[(q-xp)^2 - \Delta]^{n+1}}, \quad (26)$$

where $\Delta = -p^2 x(1-x) + (1-x)m_r^2$ and n is a positive integer. If we substitute Eq. (25) to Eq. (24), apply Eq. (26) with $n = 1$, and change the integration variables as $q - xp \rightarrow k$, we have

$$-i\Sigma_2 = i \int_0^1 dx \int \frac{d^3k}{(2\pi)^2} \gamma_\mu (\slashed{k} + x\slashed{p} - m_r)\gamma_\nu \epsilon^{\mu\nu\alpha}$$

$$\times \left(-k + p(1-x)\right)_\alpha \left[\frac{1}{[k^2 - \Delta]^2 + i\epsilon} \right.$$

$$\left. - \frac{1}{[k^2 - \Delta_\Lambda]^2 + i\epsilon} \right], \quad (27)$$

where $\Delta_\Lambda = -p^2 x(1-x) + (1-x)m_r^2 + \Lambda^2 x$. Next, we use the following identities for 2D gamma matrices:

$$\epsilon^{\mu\nu\alpha}\gamma_\mu \slashed{q}\gamma_\nu = 2ia^\alpha, \quad (28a)$$

$$\epsilon^{\mu\nu\alpha}\gamma_\mu \gamma_\nu = -2i\gamma^\alpha. \quad (28b)$$

The self-energy is then given as

$$-i\Sigma_2 = -\int_0^1 dx \int \frac{d^3k}{2\pi^2} (-k^2 + (1-x)(p^2 x + m_r \slashed{p}))$$

$$\times \left[\frac{1}{[k^2 - \Delta]^2 + i\epsilon} - \frac{1}{[k^2 - \Delta_\Lambda]^2 + i\epsilon} \right], \quad (29)$$

where we have removed the terms that are odd in k. Next, we perform a Wick rotation and obtain

$$-i\Sigma_2 = -\frac{2i}{\pi} \int_0^1 dx \int_0^\infty dk_E k_E^2 \left(k_E^2 + (1-x)\right.$$

$$\times \left(-p_E^2 x - im_r \slashed{p}_E\right)\left) \left[\frac{1}{[k_E^2 + \Delta_E]^2} \right.$$

$$\left. - \frac{1}{[k_E^2 + \Delta_{E\Lambda}]^2} \right], \quad (30)$$

where $\Delta_E = p_E^2 x(1-x) + (1-x)m_r^2$ and $\Delta_{E\Lambda} = p_E^2 x(1-x) + (1-x)m_r^2 + \Lambda^2 x$. We can evaluate the integral over k_E using

$$I_1 = \int_0^\infty dk_E k_E^4 \left[\frac{1}{[k_E^2 + \Delta_E]^2} - \frac{1}{[k_E^2 + \Delta_{E\Lambda}]^2} \right],$$

$$= \frac{3\pi}{4}(\sqrt{\Delta_{E\Lambda}} - \sqrt{\Delta_E}) \quad (31)$$

and

$$I_2 = \int_0^\infty dk_E k_E^2 \left[\frac{1}{[k_E^2 + \Delta_E]^2} - \frac{1}{[k_E^2 + \Delta_{E\Lambda}]^2} \right],$$

$$= \frac{\pi}{4}\left(\frac{1}{\sqrt{\Delta_E}} - \frac{1}{\sqrt{\Delta_{E\Lambda}}} \right). \quad (32)$$

Note that $\lim_{\Lambda \to \infty} \Delta_{E\Lambda} = \Lambda^2 x$. Finally, after undoing the Wick rotation we have

$$-i\Sigma_2 = -\frac{i}{2} \int_0^1 dx \left[-3\sqrt{\Delta} + \sqrt{x}\Lambda \right.$$

$$\left. + \frac{1}{\sqrt{\Delta}}\left(p^2 x(1-x) + \slashed{p}m_r(1-x)\right) \right], \quad (33)$$

where we clearly see the linear divergence. The counterterms will remove this divergence. We define renormalization conditions as

$$-i\Sigma(\slashed{p} = -m_r) = 0 \quad (34a)$$

$$-i\frac{d\Sigma}{d\slashed{p}}\bigg|_{\slashed{p}=-m_r} = 0, \quad (34b)$$

which fixes the location of the poles and the residue, thus the physical mass [14]. After substituting Eq. (23) to Eq. (34) we have

$$D_5 = i(\slashed{p}\delta_2 + \delta m_r)$$

$$= i\left(-\frac{1}{2}\text{sgn}(m_r)\slashed{p} + \frac{\Lambda}{3} - \frac{3}{2}|m_r| \right). \quad (35)$$

Next, we calculate D_2 which is shown in Fig. 5 and explicitly given as

$$D_2 = -\frac{1}{4}\text{tr}\left[\int \frac{d^3p}{(2\pi)^3} \frac{(i(\slashed{p} - m_r))^5}{(p^2 - m_r^2)^5 + i\epsilon}(-i\Sigma) \right], \quad (36)$$

we then substitute Eqs. (23) and (24) and Eqs. (35) and (36) perform a Wick rotation, and let $p_E \rightarrow p_E m_r$, which gives

$$D_2 = \frac{i}{8\pi^2} \frac{1}{m_r} \int_0^1 dx \int dp_E \, p_E^2 \left[\left(p_E^4 - 10p_E^2 + 5\right)\left(-p_E^2\right) \right.$$

$$\times \left(1 + \frac{(1-x)}{\sqrt{\Delta_0}}\right) - \left(5p_E^4 - 10p_E^2 + 1\right)$$

$$\times \left. \left(-3\sqrt{\Delta_0} + \frac{1-x}{\sqrt{\Delta_0}}\left(-p_E^2 x\right) + 3\right) \right] \frac{1}{(p_E^2 + 1)^5}, \quad (37)$$

where $\Delta_0 = (p_E^2 x + 1)(1-x)$. It is easy to see that the sign of D_2 depends on the combination of the sign of m_r and sign of the level of the CS term, and the same is true for all two-loop contributions to β_4. Evaluating this integral yields

$$D_2 = \frac{i}{64\pi} \frac{1}{m_r}. \quad (38)$$

In preparation for the calculation of D_3, we first need to calculate the vertex correction Γ_1, which is shown in Fig. 6

and explicitly given as

$$\Gamma_1 = = 2\pi \int \frac{d^3q}{(2\pi)^3} \frac{\gamma_\mu (i(\not{q} - m_r))^2 \gamma_\nu}{(q^2 - m_r^2)^2 + i\epsilon} \frac{\epsilon^{\mu\nu\alpha}(p-q)_\alpha}{(p-q)^2 + i\epsilon}. \quad (39)$$

Here, if we check the superficial degree of divergence of Γ_1 by counting the net order of q, we naively find a logarithmic UV divergence. However, this is not the actual case, because the leading term of the integrand is an odd function of q. As a result, the naive logarithmically divergent term has zero coefficient, and the integral in Eq. (39) actually converges. We apply Eq. (26) with $n = 2$, change the integration variables as $q - xp \to k$, and obtain

$$\Gamma_1 = -4\pi \int_0^1 dx \int \frac{d^3k}{(2\pi)^3} \gamma_\mu (\not{k} + x\not{p} - m_r)^2 \gamma_\nu \epsilon^{\mu\nu\alpha}$$

$$\times \left(-k + p(1-x)\right)_\alpha \left[\frac{1-x}{[k^2 - \Delta]^3 + i\epsilon}\right]. \quad (40)$$

After using Eq. (28) and removing the odd terms in k, we have

$$\Gamma_1 = i8\pi \int_0^1 dx \int \frac{d^3k}{(2\pi)^3} \left[\not{p}(1-x)(k^2 + x^2p^2 + m_r^2)\right.$$

$$- \not{k}(2xp \cdot k) + 2m_r(-k^2 + (1-x)xp^2)\right]$$

$$\times \left[\frac{1-x}{[k^2 - \Delta]^3 + i\epsilon}\right]. \quad (41)$$

Now it is clear that this integral is not divergent, because the term that would produce logarithmic UV divergence is canceled as a result of the removal of the odd terms. We can further simplify this by making the following substitution:

$$\not{k}(p \cdot k) \to \tfrac{1}{3} k^2 \not{p}, \quad (42)$$

which is a result of the symmetry of the integral in k. Then, we perform a Wick rotation:

$$\Gamma_1 = 8\pi \int_0^1 dx \int \frac{d^3k_E}{(2\pi)^3} \left[-i\not{p}_E(1-x)\left(-k_E^2 - x^2p_E^2\right.\right.$$

$$\left. + m_r^2\right) - \frac{2k_E^2 \not{p}_E}{3}$$

$$+ 2m_r\left(k_E^2 - (1-x)xp_E^2\right)\right]\left[\frac{1-x}{\left[k_E^2 + \Delta_E\right]^3}\right]. \quad (43)$$

We can evaluate the integral over k_E using the integral identities given in Appendix. We have

$$\Gamma_1 = \frac{1}{4}\int_0^1 dx(1-x)\left[\frac{3(i\not{p}_E(1-5x/3) + 2m_r)}{\sqrt{\Delta_E}}\right.$$

$$\left. + \frac{(m_r^2 - x^2p_E^2)(1-x)(-i\not{p}_E) - 2m_r x(1-x)p_E^2}{\Delta_E^{3/2}}\right]. \quad (44)$$

Finally, we can calculate D_3, which is shown in Fig. 5 and explicitly given as

$$D_3 = -\frac{1}{4}\text{tr}\left[\int \frac{d^3p}{(2\pi)^3} \frac{(i(\not{p} - m_r))^4}{(p^2 - m_r^2)^4 + i\epsilon} \Gamma_1\right]. \quad (45)$$

As before, we make the Wick rotation, let $p_E \to p_E m_r$, and substitute Γ_1, which gives

$$D_3 = -\frac{i}{16\pi^2}\frac{1}{m_r}\int_0^1 dx \int_0^\infty dp_E p_E^2 \left[-p_E^2\left(\frac{3-5x}{\sqrt{\Delta_0}}\right.\right.$$

$$\left.- \frac{(1-x)(1-x^2p_E^2)}{\Delta_0^{3/2}}\right)(-4p_E^2 + 4)$$

$$+ \left(\frac{6}{\sqrt{\Delta_0}} - \frac{2(1-x)xp_E^2}{\Delta_0^{3/2}}\right)(p_E^4 - 6p_E^2 + 1)\right]$$

$$\times \frac{1-x}{\left(p_E^2 + 1\right)^4}. \quad (46)$$

Evaluating this integral yields

$$D_3 = 0. \quad (47)$$

Next we calculate D_4. First, we start with Γ_2, which is shown in Fig. 6 and explicitly given as

$$\Gamma_2 = 2\pi \int \frac{d^3q}{(2\pi)^3} \frac{\gamma_\mu (i(\not{q} - m_r))^3 \gamma_\nu}{(q^2 - m_r^2)^3 + i\epsilon} \frac{\epsilon^{\mu\nu\alpha}(p-q)_\alpha}{(p-q)^2 + i\epsilon}, \quad (48)$$

which is convergent. First, we apply Eq. (26) with $n = 3$ and change the integration variables as $q - xp \to k$ and we have

$$\Gamma_2 = -i6\pi \int_0^1 dx \int \frac{d^3k}{(2\pi)^3} \gamma_\mu (\not{k} + x\not{p} - m_r)^3 \gamma_\nu \epsilon^{\mu\nu\alpha}$$

$$\times (-k + p(1-x))_\alpha \left[\frac{(1-x)^2}{[k^2 - \Delta]^4 + i\epsilon}\right]. \quad (49)$$

Next, we simplify the gamma matrix terms by using Eqs. (28) and show that

$$\epsilon^{\mu\nu\alpha}\gamma_\mu (\not{k} + x\not{p} - m_r)^3 \gamma_\nu(-k + p(1-x))_\alpha$$

$$= 2i(k^2 + x^2p^2 + 2xk \cdot p + 3m_r^2)(k + xp)$$

$$\cdot (-k + p(1-x)) + (-\not{k} + \not{p}(1-x))$$

$$\times \left[3(k^2 + x^2p^2 + 2xp \cdot k) + m_r^2\right]2im_r, \quad (50)$$

then, we apply Eq. (42) and a Wick rotation, so Γ_2 becomes

$$\Gamma_2 = 12i\pi \int_0^1 dx \int \frac{d^3k_E}{(2\pi)^3}\left(\left(k_E^2 - p_E^2 x(1-x)\right)\right.$$

$$\times \left(-k_E^2 - x^2p_E^2 + 3m_r^2\right) + \frac{2x}{3}p_E^2 k_E^2(1-2x)$$

$$- im_r 2xk^2 \not{p}_E - im_r \not{p}_E(1-x)\left(3\left(-k_E^2 - x^2p_E^2\right) + m_r^2\right)\right)$$

$$\times \left[\frac{(1-x)^2}{\left[k_E^2 + \Delta_E\right]^4}\right]. \quad (51)$$

We can evaluate the integral over k_E using the integral identities given in Appendix. Γ_2 is now

$$\Gamma_2 = \frac{3i}{16} \int_0^1 dx(1-x)^2 \left[\frac{-5}{\Delta_E^{1/2}} + \frac{1}{\Delta_E^{3/2}} \left(\frac{5x}{3} p_E^2(1-2x) \right. \right.$$
$$+ 3m_r^2 + im_r \not{p}_E(3-5x) \bigg) + \frac{1}{\Delta_E^{5/2}} \left(-p_E^2 x(1-x) \right.$$
$$\left. \times \left(-x^2 p_E^2 + 3m_r^2\right) - im_r \not{p}_E(1-x)\left[-3x^2 p_E^2 + m_r^2 \right] \right) \bigg].$$
$$(52)$$

Finally, we can calculate D_4 which is shown in Fig. 5 and explicitly given as

$$D_4 = -\frac{1}{4} \text{tr} \left[\int \frac{d^3 p}{(2\pi)^3} \frac{(i(\not{p} - m_r))^3}{(p^2 - m_r^2)^3 + i\epsilon} (\Gamma_2) \right]. \quad (53)$$

As before we make Wick rotation, let $p_E \to p_E m_r$ and substitute Γ_2 which gives

$$D_4 = -\frac{3i}{64\pi^2} \frac{1}{m_r} \int_0^1 dx \int_0^\infty dp_E p_E^2 \frac{(1-x)^2}{(p_E+1)^3}$$
$$\times \left\{ -p_E^2(-p_E^2+3) \left(\frac{3-5x}{\Delta_0^{3/2}} - (1-x)\frac{-3x^2 p_E^2+1}{\Delta_0^{5/2}} \right. \right.$$
$$+ (1 - 3p_E^2) \left[\frac{-5}{\Delta_0^{1/2}} + \frac{1}{\Delta_0^{3/2}} \left(\frac{5x}{3} p_E^2(1-2x) + 3 \right) \right.$$
$$\left. \left. + \frac{1}{\Delta_0^{5/2}} \left(-p_E^2 x(1-x)(-x^2 p_E^2+3) \right) \right] \right) \right\}. \quad (54)$$

If we evaluate this numerically, we have

$$D_4 = -\frac{i}{32\pi} \frac{1}{m_r}. \quad (55)$$

Finally, we get β_4 by using Eqs. (37), (46), and (54), which gives

$$\beta_4 = -\frac{1}{64\pi} \frac{1}{m_r}, \quad (56)$$

which is the main result of this section.

We now discuss three different cases.

(i) $m_r > 0$. This describes a CSL phase. Since $\beta_4 > 0$, its transition into the phase with VBS and/or Ising Neel order is first order at the mean-field level.

(2) $m_r < 0$. This describes an XY phase. Since $\beta_4 < 0$, its transition into the phase with VBS and/or Ising Neel order is second order at the mean-field level.

It should be noted that our evaluation of β_4 is only to the lowest order in gauge coupling (or inverse CS level), which is of order one. We cannot rule out the possibility that higher order correction can reverse the sign of β_4 and thus the conclusions above.

(3) $m_r = 0$. This is our multicritical point, at which we cannot integrate out the (massless) Dirac fermions perturbatively as done above. One can, nevertheless, perform a nonperturbative calculation of the effective potential [14] $V_{\text{eff}}(\phi_{\text{cl}})$ in terms of ϕ_{cl}, which is the vacuum expectation value of ϕ where $V_{\text{eff}}(\phi_{\text{cl}})$ is minimized. Since the fermion theory is massless and contains no scale, one expects its coupling to ϕ_{cl} generates a scale-invariant term $|\phi_{\text{cl}}|^3$, which is easy to verify by calculating the change of fermion ground-state energy due to ϕ_{cl} that plays the role of a mass. The nonanalyticity of such a term originates from the masslessness of the Dirac fermion. Its presence signals the non-mean-field behavior of the transition into the phases with broken translation symmetry, even if the theory is analyzed at the mean-field level.

V. DUAL DESCRIPTION

The theory of multicritical point is also discussed in Ref. [22], which is mainly done by considering a mean-field approach by considering the dual version of the theory. Thus, to have a connection with the literature, we also briefly find a dual version of our theory. In Sec. II, we started with the lattice spin model given in Eq. (2), then we mapped it to hard-core bosons, and then mapped those hard-core bosons to nonrelativistic fermions in a lattice with a level-one CS term. Then, we found that the continuum limit of this theory is described by two Dirac fermions coupled to the level-one CS term given in Eq. (5). In this section, we will apply a bosonization transformation to Eq. (5), which, in a sense, close the circle of our mappings.

We will use the well-known bosonization conjecture [11,15–19]. First, we have to make several definitions to simplify the notation in the following calculations. We closely follow the approach of Ref. [15] in this section. We define the CS term and background field coupling as [15]

$$S_{\text{CS}}[a] = \frac{1}{4\pi} \int d^3 x \epsilon^{\mu\nu\lambda} a_\mu \partial_\nu a_\lambda, \quad (57a)$$

$$S_{\text{BF}}[a, B] = \frac{1}{2\pi} \int d^3 x \epsilon^{\mu\nu\lambda} a_\mu \partial_\nu B_\lambda, \quad (57b)$$

where a is a dynamic gauge field and B is a background gauge field—note that we use lower case letters for dynamic gauge fields and upper case letters for background-gauge fields as before. The actions for material fields are given as

$$S_{\text{fermion}}[\psi, A] = \int d^3 x \bar{\psi} (i(\gamma^\mu \partial_\mu - iA_\mu)\psi, \quad (58a)$$

$$S_{\text{scalar}}[\phi, A] = \int d^3 x |(\partial_\mu - iA_\mu)\phi|^2 - \alpha|\phi|^4, \quad (58b)$$

where we have an action for a free Dirac fermion coupled to the background gauge field and complex Wilson-Fischer (WF) scalar, with coupling constant α which flows to infinity at the WF fixed point and the mass flows to zero [15]. Their partition functions

$$Z_{\text{fermion}}[A] = \int \mathcal{D}\bar{\psi}\mathcal{D}\psi e^{iS_{\text{fermion}}[\psi,A]}, \quad (59a)$$

$$Z_{\text{scalar}}[A] = \int \mathcal{D}\bar{\phi}\mathcal{D}\phi e^{iS_{\text{scalar}}[\phi,A]} \quad (59b)$$

are related by the bosonization conjecture [15]:

$$Z_{\text{fermion}}[A] e^{-\frac{i}{2}S_{\text{CS}}[A]} = \int \mathcal{D}a Z_{\text{scalar}}[a] e^{iS_{\text{CS}}[a]+iS_{\text{BF}}[a;A]}. \quad (60)$$

We have to clarify the origin of the extra half-level CS term on the left-hand side (LHS), which is something purely notational. To understand this, assume for a moment the fermions in LHS are massive. In our notation, when we integrate out the fermions of $Z_{fermion}[A]$, we do not perform any Pauli-Villars regularization [20] and, as a result of that, we get a half-level CS term after integrating out the fermions. However, a CS term with a noninteger level breaks the large gauge invariance [20]. So, to preserve the gauge invariance of the theory, we have to add that extra half-level CS term [21].

Our goal is to obtain Eq. (5) by applying a series of manipulations to LHS of Eq. (60). Applying the same manipulations to the right-hand side (RHS) of Eq. (60) yields the dual (or bosonized) version of Eq. (5).

First, we multiply two copies of the LHS of Eq. (60) and integrate it over A. We denote this integration variable as $\tilde{a}$ and add a coupling with background field C. So, the theory becomes

$$S_L = S_f[\psi_1, \tilde{a}] + S_f[\psi_2, \tilde{a}] - S_{BF}[\tilde{a}, C] - S_{CS}[\tilde{a}], \quad (61)$$

which gives the fermionic side of our new duality. Performing the same manipulations to the RHS of Eq. (60) yields

$$S_R = S_s[\phi_1, a_1] + S_s[\phi_2, a_2] + S_{CS}[a_1] + S_{CS}[a_2] \\ + S_{BF}[a_1 + a_2 - C, \tilde{a}], \quad (62)$$

and this is the bosonic side of our new duality. Next, we integrate out $\tilde{a}$ on the RHS, which gives rise to the constraint

$$C = a_1 + a_2, \quad (63)$$

which we solve by introducing a new dynamic field b as $a_1 = b$ and $a_2 = -b + C$. Then S_R becomes

$$S_R = S_s[\phi_1, b+] + S_s[\phi_2, -b + C] + S_{CS}[b] + S_{CS}[-b + C]. \quad (64)$$

Next, we apply time reversal transformation to both sides by simply changing the signs of the BF and CS terms. We then have

$$S'_L = S_f[\psi_1, \tilde{a}] + S_f[\psi_2, \tilde{a}] + S_{BF}[\tilde{a}, C] + S_{CS}[\tilde{a}]. \quad (65)$$

The motivation behind this transformation is clear, as the fermionic theory now contains a level-one CS term as in Eq. (5). Accordingly, the bosonic side of the duality is

$$S'_R = S_s[\phi_1, b] + S_s[\phi_2, -b + C] - S_{CS}[b] - S_{CS}[-b + C]. \quad (66)$$

Next, we let $C \to -C$ and we add $S_{CS}[C]$ to both sides. So, both sides of the duality are given as

$$S''_L = S_f[\psi_1, \tilde{a}] + S_f[\psi_2, \tilde{a}] + S_{CS}[\tilde{a} - C]. \quad (67)$$

Note that for $C = A$ this is just the action of Eq. (5) and the bosonic side of the duality is

$$S''_R = S_s[\phi_1, b] + S_s[\phi_2, -b - C] \\ - 2S_{CS}[b] - S_{BF}[b, C]. \quad (68)$$

Finally, we let $\phi_2 \leftrightarrow \phi_2^*$ and get

$$S'''_R = S_s[\phi_1, b] + S_s[\phi_2, b + C] \\ - 2S_{CS}[b] - S_{BF}[b, C], \quad (69)$$

which concludes the bosonization of Eq. (5). One should note that this is not the only possible duality that one can find. For example, we can find different bosonic dual models to our original model by considering the time-reversed version of Eq. (60) to the one of the fermionic degrees of freedom in our original model.

VI. SUMMARY AND DISCUSSION

In this paper, we provide a unified description of various possible phases supported by a spin-$\frac{1}{2}$ antiferromagnet with easy-plane anisotropy on the square lattice, including Neel-order states, CSL, and VBSs. The description is based on two Dirac fermions coupled to a level-one CS gauge field, and the various phases correspond to different combinations of the various Dirac mass terms. All these phases meet at a multicritical point where the entire Dirac mass matrix vanishes. Within our description, a direct continuous transition from the XY-ordered Neel state to the VBS must go through this multicritical point. In more generic situations, there is either an intermediate phase with both orders or a direct first-order transition.

The theory of this multicritical point and its dual description have some similarities to that of the deconfined criticality [3] and its dual description [22]. The main difference is our models contain CS couplings while their models do not. As a result, their phase diagram does not contain the CSL phase.

APPENDIX: INTEGRAL IDENTITIES

Here we discuss the common integrals we will encounter in the main text [14],

$$\int \frac{d^d k_E}{(2\pi)^d} \frac{1}{\left[k_E^2 + \Delta_E\right]^n} \\ = \frac{1}{(4\pi)^{d/2}} \frac{\Gamma(n - \frac{d}{2})}{\Gamma(n)} \left(\frac{1}{\Delta_E}\right)^{n - \frac{d}{2}}, \quad (A1a)$$

$$\int \frac{d^d k_E}{(2\pi)^d} \frac{k_E^2}{\left[k_E^2 + \Delta_E\right]^n} \\ = \frac{d}{2(4\pi)^{d/2}} \frac{\Gamma(n - \frac{d}{2} - 1)}{\Gamma(n)} \left(\frac{1}{\Delta_E}\right)^{n - \frac{d+2}{2}}, \quad (A1b)$$

$$\int \frac{d^d k_E}{(2\pi)^d} \frac{k_E^4}{\left[k_E^2 + \Delta_E\right]^n}$$

$$= \frac{d(d/2+1)}{2(4\pi)^{d/2}} \frac{\Gamma\left(n - \frac{d}{2} - 2\right)}{\Gamma(n)} \left(\frac{1}{\Delta_E}\right)^{n - \frac{d+4}{2}}, \quad \text{(A1c)}$$

where $n \in \mathbb{Z}^+$, which can be proved easily by converting the LHS to the Euler integral (beta function) by substituting $x = \Delta_E/(k_E^2 + \Delta_E)$.

[1] C. Broholm, R. J. Cava, S. A. Kivelson, D. G. Nocera, M. R. Norman, and T. Senthil, Quantum spin liquids, Science **367**, eaay0668 (2020).

[2] S. M. Girvin and K. Yang, *Modern Condensed Matter Physics* (Cambridge University Press, UK, 2019).

[3] T. Senthil, L. Balents, S. Sachdev, A. Vishwanath, and M. P. A. Fisher, Quantum criticality beyond the Landau-Ginzburg-Wilson paradigm, Phys. Rev. B **70**, 144407 (2004).

[4] B. Zhao, J. Takahashi, and A. W. Sandvik, Multicritical Deconfined Quantum Criticality and Lifshitz Point of a Helical Valence-Bond Phase, Phys. Rev. Lett. **125**, 257204 (2020).

[5] N. Desai and R. K. Kaul, First-order phase transitions in the square-lattice easy-plane J-Q model, Phys. Rev. B **102**, 195135 (2020).

[6] A. Lopez, A. G. Rojo, and E. Fradkin, Chern-Simons theory of the anisotropic quantum Heisenberg antiferromagnet on a square lattice, Phys. Rev. B **49**, 15139 (1994).

[7] One for each Dirac point, and they each have two components representing the A and B sublattice. Note a rotation is performed on one of the Dirac points so the two Dirac fields have the same chirality which allows for a unified description in Eq. (5).

[8] M. Barkeshli and J. McGreevy, Continuous transition between fractional quantum Hall and superfluid states, Phys. Rev. B **89**, 235116 (2014).

[9] K. Yang, L. K. Warman, and S. M. Girvin, Possible Spin-Liquid States on the Triangular and Kagomé Lattices, Phys. Rev. Lett. **70**, 2641 (1993).

[10] V. Shyta, J. van den Brink, and F. S. Nogueira, Deconfined Criticality and Bosonization Duality in Easy-Plane Chern-Simons Two-Dimensional Antiferromagnets, Phys. Rev. Lett. **127**, 045701 (2021).

[11] T. Senthil, D. T. Son, C. Wang, and C. Xu, Duality between (2 + 1)d quantum critical points, Phys. Rep. **827**, 1 (2019).

[12] There are other possible four external leg and two-loop, irreducible diagrams with one photon propagator. We find those diagrams to be zero under an appropriate regularization scheme.

[13] W. Chen, M. P. A. Fisher, and Y. S. Wu, Mott transition in an anyon gas, Phys. Rev. B **48**, 13749 (1993).

[14] M. E. Peskin and D. V. Schroeder, *An Introduction to Quantum Field Theory* (Westview, Boulder, CO, 1995), includes exercises.

[15] A. Karch, B. Robinson, and D. Tong, More Abelian dualities in 2 + 1 dimensions, J. High Energy Phys. 01 (2017) 017.

[16] A. Karch and D. Tong, Particle-Vortex Duality from 3D Bosonization, Phys. Rev. X **6**, 031043 (2016).

[17] N. Seiberg, T. Senthil, C. Wang, and E. Witten, A duality web in 2 + 1 dimensions and condensed matter physics, Ann. Phys. **374**, 395 (2016).

[18] J. H. Son, J. Y. Chen, and S. Raghu, Duality web on a 3D Euclidean lattice and manifestation of hidden symmetries, J. High Energy Phys. 06 (2019) 038.

[19] J. Chen, J. Son, C. Wang, and S. Raghu, Exact Boson-Fermion Duality on a 3D Euclidean Lattice, Phys. Rev. Lett. **120**, 016602 (2018).

[20] D. Tong, Lectures on the gauge theory (2018), http://www.damtp.cam.ac.uk/user/tong/gaugetheory/gt.pdf.

[21] We could have used an alternative notation such that when we integrate out the fermions in $Z_f[A]$, we could have performed Pauli-Villars regularization. In that case, Pauli-Villars regularization would automatically add that extra half-level CS term which would eliminate to necessity of adding it by hand. However, in his paper we don't use this notation.

[22] C. Wang, A. Nahum, M. A. Metlitski, C. Xu, and T. Senthil, Deconfined Quantum Critical Points: Symmetries and Dualities, Phys. Rev. X **7**, 031051 (2017).